Revision of the energy calibration of the Yakutsk extensive air shower array

A. V. Glushkov, M. I. Pravdin, and A. Sabourov[*]

Yu. G. Shafer Institute of Cosmophysical Research and Aeronomy,
Lenin Avenue 31, 677980 Yakutsk, Russia

Responses of surface and underground scintillation detectors of Yakutsk array are calculated for showers initiated by primary particles with energy $E_0 \geq 10^{17}$ eV within the frameworks of QGSJet01d, QGSJet-II-04, SIBYLL-2.1, and EPOS-LHC hadron interaction models. A new estimation of E_0 is obtained with the use of various methods. The resulting energy is lower compared to the obtained with earlier method by a factor of ~1.33.

PACS numbers: 96.50.sb, 96.50.sd

I. INTRODUCTION

Energy spectrum of ultrahigh energy cosmic rays (UHECRs), cosmic rays (CRs) with $E_0 \geq 10^{17}$ eV energy, is one of the main links in the chain of complex problems associated with understanding the nature of primary particles with such energy. Mechanisms of their production and acceleration in astrophysical sources and various effects they experience during the propagation in the Universe have a direct effect on the observed primary CR spectrum. Recently, significant progress has been achieved in interpretation of its structural features in the ultrahigh energy domain. The blackbody cutoff at $E_0 \sim 6 \times 10^{19}$ eV predicted by Greisen [1] and Zatsepin and Kuz'min [2] (the GZK cutoff) has been confirmed [3,4], thus pointing at extragalactic origin of the most energetic CR particles. The second knee (at $\sim 10^{17}$ eV) and the ankle (at $\sim 10^{18}$ eV) are commonly associated with a transition between galactic and extragalactic CR components, and although its exact location on the energy scale is not known precisely, there are plenty of theoretical scenarios compatible with existing experimental observations (e.g., [5–7]).

However, there is certain discrepancy in the world array of experimental results. CR spectra measured by various UHECR experiments [8–12] confirm such spectral features as the ankle and the second knee, but they differ from each other in absolute intensity by a factor of almost 2 [13,14]. In particular, the spectrum measured by the Yakutsk experiment lies above all the world data. In this context, the data published by the Yakutsk group signify the upper limit of the spectrum intensity, and data from the Pierre Auger Observatory (PAO) signify its lower limit.

Such a situation to a large extent stems from the fact that the only available method of UHECR observation is indirect, conducted by registering cascades of secondary particles produced by primary UHECRs in the Earth's atmosphere: extensive air showers (EASs). Most of the largest experiments employ differing observational techniques and, consequently, rely on different methods to reconstruct the energy of primary particles. Hence, one cannot do without the theoretical notion of EAS development.

The Yakutsk EAS array stands out from other large arrays for its complexity: since it is equipped with detectors of three types, it simultaneously registers several shower components. Charged particles (electrons, positrons, and muons) are recorded with 2-m² surface scintillation detectors (SSDs). Muon component arising from nuclear interactions is registered with detectors of the same type placed below the ground level, in order to prevent electromagnetic contamination by creating a shield with $1 \times \sec \theta$ GeV threshold. Cherenkov light emitted by EAS charged particles is recorded with integral Cherenkov detectors based on the FEU-49 photomultiplier tube.

Cherenkov component carries information about ~80% of primary energy dissipated in the atmosphere and thus enables us to determine E_0 with the calorimetric method [15–19]. This method defines the E_0 as a sum of energies of all EAS components and connects it with the experimentally measured value $\rho_{s,600}$ (it is discussed in greater detail in Sec. III). Originally, it was introduced in [20] for energies $\sim 10^{15}$ eV. In the Yakutsk experiment, it was applied to showers with $E_0 \simeq (1.0–100) \times 10^{17}$ eV at zenith angles $\theta \leq 45°$ [15,16] and resulted in the following approximation for primary energy reconstruction:

$$E_0 = (4.1 \pm 1.4) \times 10^{17} \cdot (\rho_{s,600}(0°))^{0.97 \pm 0.04} \text{ (eV)}, \quad (1)$$

$$\rho_{s,600}(0°) = \rho_{s,600}(\theta) \times \exp\left(\frac{(\sec\theta - 1) \cdot x_0}{\lambda_\rho}\right), \quad (2)$$

$$\lambda_\rho = 400 \pm 45 \text{ (g/cm}^2), \quad (3)$$

where $x_0 = 1020$ g/cm², $\rho_{s,600}(\theta)$ is the density of charged particles (m⁻²) measured by SSDs at the distance $R = 600$ m from shower axis, and λ_ρ is attenuation length. Later, the relations (1) and (3) were changed slightly (see [17–19]):

[*]tema@ikfia.sbras.ru

$$E_0 = (4.8 \pm 1.6) \times 10^{17} \cdot (\rho_{s,600}(0°))^{1.0 \pm 0.02}, \quad (4)$$

$$\lambda_\rho = (450 \pm 44) + (32 \pm 15) \cdot \log_{10} \rho_{s,600}(0°). \quad (5)$$

The intensity of the CR energy spectrum estimated with the use of (4) turned out to be significantly higher than the world data (see, e.g., [21]). In [22], estimation of E_0 for Yakutsk data was presented obtained for primary protons within the framework of QGSJet01 model, which was 1.6 times lower than (4). Here we consider energy calibration of registered showers based on modern CORSIKA code (version 6.7370) [23].

II. LATERAL DISTRIBUTION OF THE DETECTOR SIGNAL

Basic EAS parameters measured in the Yakutsk experiment (arrival direction, coordinates of the shower axis, primary energy) are reconstructed with lateral distribution function (LDF) of all particles (electrons, muons, and high-energy photons), which are registered by SSDs. These particles pass through a multilayer shield consisting of snow, iron, wood, and aluminum (total thickness amounts to ~2.5 g/cm^2) and then through a 5-cm thick scintillator (with the density ~1.06 g/cm^3). The energy deposit in a scintillator $\Delta E_s(R)$ is proportional to the number of particles passed though a detector and is measured in relative units:

$$\rho_s(R) = \frac{\Delta E_s(R)}{E_1} (\text{m}^{-2}), \quad (6)$$

where $E_1 = 11.75$ MeV, which is the energy released in a scintillator during the passage of a vertical relativistic muon (the response unit).

Scintillation detectors are calibrated and controlled with the use of amplitude density spectra from background cosmic particles [24]. Herewith, the integral spectra of two types are used. The first one is a spectrum from a single detector, which is controlled by a nearby detector mounted in the same station [the so-called spectrum of double coincidence with the frequency $\simeq (2–3)$ s^{-1}]. The second one is an uncontrolled spectrum with the frequency ~200 s^{-1}, which is used to calibrate muon detectors. Both spectra are described by a power law:

$$F(> \rho) \sim \rho^{-\eta} \sim U^{-\eta}, \quad (7)$$

where values of η for both spectra were obtained experimentally. For spectrum of the first type $\eta = 1.7$ and for spectrum of the second type, $\eta = 3.1$. $\rho = U/U_1$; particle density is measured in units of signal amplitude U_1 from a reference detector during the passage of a vertical relativistic cosmic muon. The procedure of calibration and control consists of continual monitoring of the U_1 value in all detectors by periodical measurements of their density

spectra. The procedure is performed once every two days. Spectra of double coincidence are collected for two hours, uncontrolled spectra for 30 minutes.

Within the framework of models QGSJet01d [25], QGSJet-II-04 [26], SIBYLL-2.1 [27], and EPOS-LHC [28], we calculated LDF of the SDD response in showers, initiated by primary protons and iron nuclei with energies $10^{17.0}–10^{19.5}$ eV arriving at different zenith angles. FLUKA package [29,30] was chosen for treatment of lower energy interactions. At first, the response $u_m(\epsilon, \theta)$ from a single particle of a type m (where m is electron, muon, or gamma photon) with energy ϵ was calculated. During the calculation, all the main processes occurring in the detector during energy release/consumption with corresponding cross sections were put into consideration: ionization and bremsstrahlung for charged particles and pair production and delta electrons from Compton effect for gamma photons. Then the development of air shower was simulated with CORSIKA code. For each set of primary parameters (mass of primary particle, its energy, and incident zenith angle), 500 showers were simulated. In order to speed up the simulation, the "thin-sampling" mechanism, introduced in [31], was activated in the CORSIKA code [23,32]. The thinning level $\epsilon_{th} = \epsilon_{min}/E_0$, controlling the minimal energy of secondary particles ϵ_{min} treated by CORSIKA, was defined in the interval 3.16×10^{-6}, 10^{-5} and the weight limit of secondary particles w_{max} was in the interval 10^4, 3.16×10^6, depending on the primary energy. This was done in order to limit the growth of artificial fluctuations induced by thin sampling in showers with lower energies.

During conversion to density, the number of particles was calculated in the detector of a given area. Resulting showers were averaged together, and mean energy spectra $d_m(\epsilon, R, \theta)$ were calculated for all particle types in intervals $(\log_{10} R_j, \log_{10} R_j + 0.04)$. The signal (6) at a distance R was defined as a sum of responses:

$$\rho_s(R) = \sum_m^3 \sum_{i=1}^{I_m} u_m(\epsilon_i, \theta_i) d_m(\epsilon_i, R, \theta_i), \quad (8)$$

where I_m is the number of particles of a type m hitting a detector at a distance R.

In Fig. 1, the dependence of the value $\log_{10}[\rho_{s,600}(0°)/E_0]$ from E_0 is shown for primary protons (open circles) and iron nuclei (black circles), as predicted by the QGSJet01d model. They satisfy the relation

$$E_0 = (3.24 \pm 0.1) \times 10^{17} \cdot (\rho_{s,600}(0°))^{1.015}. \quad (9)$$

Other models—QGSJet-II-04, SIBYLL-2.1, and EPOS-LHC—give the following estimations correspondingly:

$$E_0 = (3.52 \pm 0.1) \times 10^{17} \cdot (\rho_{s,600}(0°))^{1.02}, \quad (10)$$
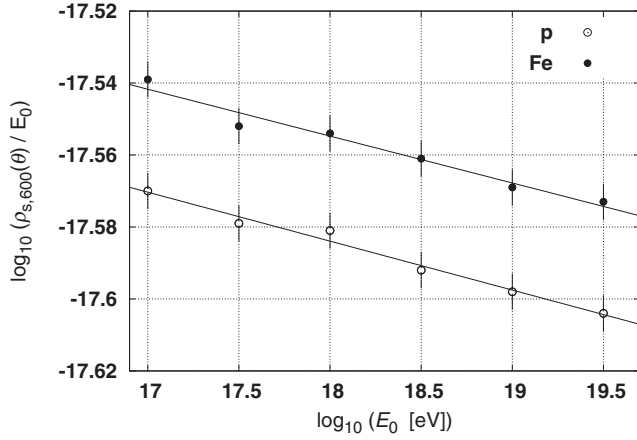
FIG. 1. Energy dependence of $\log_{10}[\rho_{s,600}(\theta)/E_0]$ for primary protons and iron nuclei according to predictions of QGSJet01d for vertical showers.

$$E_0 = (3.09 \pm 0.1) \times 10^{17} \cdot (\rho_{s,600}(0°))^{1.015}, \quad (11)$$

$$E_0 = (3.74 \pm 0.1) \times 10^{17} \cdot (\rho_{s,600}(0°))^{1.02}. \quad (12)$$

Averaging over all models gives the dependence

$$E_0 = (3.40 \pm 0.18)^{17} \cdot (\rho_{s,600}(0°))^{1.017}, \quad (13)$$

which resulted in a lower estimated value of E_0 by factor 1.20 when compared to (1) and by 1.41 when compared to (4).

Zenith-angular dependencies of $\log_{10}(\rho_{s,600}(\theta)/E_0)$ according to QGSJet01d model are shown on Fig. 2. They satisfy a linear dependency with $\lambda_\rho = 415 \pm 15$ g/cm^2 at any composition of primary CR when $\sec\theta$ is lesser than

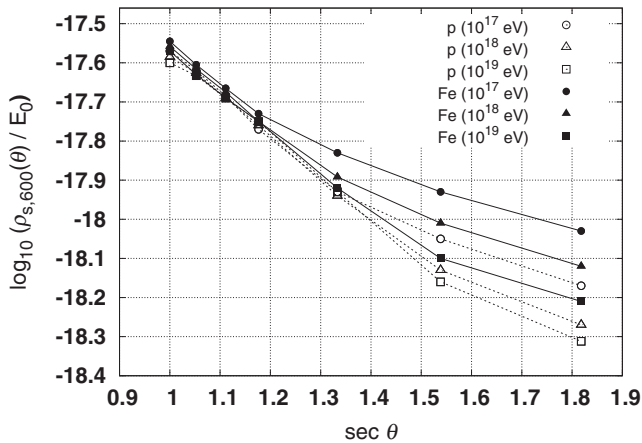$$\sec\theta_{\lim} = a + b \log \rho_{s,600}(\theta), \quad (14)$$

FIG. 2. Zenith-angular dependence of $\log_{10}[\rho_{s,600}(\theta)/E_0]$ according to QGSJet01d predictions for protons and iron nuclei with energy $E_0 = 10^{17}$, 10^{18}, and 10^{19} eV.

where $a = 1.26$ and $b = 0.077$. In the case of protons, the relation (14) is agreeable for inclined showers with $a = 1.477$, at $E_0 = 10^{19}$ eV, with attenuation length $\lambda_\rho = 415$ g/cm^2 and for $\theta \le 50°$. In other cases, the dependency is more complex.

III. CALORIMETRIC METHOD

We considered the energy balance starting from the example of experimental data from [15,16]. Earlier, these data had provided a basis for the calorimetric method of E_0 estimation adopted for the Yakutsk array. The observables and main components constituting the primary energy are given in Tables I and II for $E_0 = 10^{18}$ eV and $\cos\theta = 0.95$. The F column in the Table I is the flux of Cherenkov photons measured with integral Cherenkov light detectors. The values for k_γ and $k_{\rm ion}$ in the same table were obtained in simulation with CORSIKA. Mean values of N_s and N_μ were obtained from the LDFs averaged over energy interval. The row entitled "average p-Fe" corresponds to values averaged over all models and compositions. The energy dissipated in the atmosphere by electromagnetic component equals to

$$E_i = E_\gamma + E_{\rm ion}, \quad (15)$$

where E_γ is energy of gamma photons on observation level and $E_{\rm ion}$ is summary ionization losses of all electrons and positrons. It is proportional to the total flux F of Cherenkov radiation in the atmosphere:

$$E_i = k \cdot F, \quad (16)$$

where k (eV/photon eV^{-1}) is the scaling factor:

$$k = k_\gamma + k_{\rm ion} = \frac{E_\gamma + E_{\rm ion}}{F}. \quad (17)$$

On Fig. 3, the dependence of the scaling factor (17) from the path from $x_{\max}$ to observation level ($x_{\rm obs} = x_0 \times \sec\theta$ g/cm^2) is shown. The flux F is determined with respect to its attenuation by factor 1.15 due to Rayleigh scattering in clean atmosphere and degradation of the relative transparency in sampling events [15,16] by a factor of 1.1. It is given for radiation interval 1 eV:

$$F = \frac{1.265 F_{\rm obs}}{\Delta\epsilon}, \quad (18)$$

where $F_{\rm obs}$ is the flux measured in experiment with integral Cherenkov light detectors and

$$\Delta\epsilon = 12400 \cdot \left(\frac{1}{\lambda_1} - \frac{1}{\lambda_2}\right) \simeq 2.58 \text{ (eV)}. \quad (19)$$

Here $\lambda_1 = 3000$ Å, $\lambda_2 = 8000$ Å. The energy $E_{\rm el}$ is the amount of primary energy carried by electrons and

TABLE I.   Observables of EAS with $E_0 = 10^{18}$ eV and $\cos\theta = 0.95$ from primary nuclei (A) according to CORSIKA [23] simulation and experiment [16].

Model	A	$k_\gamma(\theta)$ $(\times 10^4)$ eV^2	$k_{\text{ion}}(\theta)$ $(\times 10^4)$ eV^2	$F(\theta)$ $(\times 10^{13})$ eV^{-1}	$\langle N_s(\theta)\rangle$ $(\times 10^8)$	$\rho_{s,600}(\theta)$ m^{-2}	$\langle N_\mu(\theta)\rangle$ $(\times 10^6)$
QGSJet01d	p	0.341	2.846	2.104	2.178	2.312	5.000
	Fe	0.224	2.910	2.148	1.250	2.432	7.225
QGSJet-II-04	p	0.364	2.816	2.070	2.296	2.438	5.582
	Fe	0.246	2.894	2.148	1.358	2.636	7.777
SIBYLL-2.1	p	0.345	2.822	2.100	2.512	2.193	4.254
	Fe	0.224	2.910	2.228	1.384	2.249	4.930
EPOS-LHC	p	0.377	2.815	2.023	2.355	2.655	5.905
	Fe	0.230	2.894	2.133	1.419	2.917	8.180
	p	0.357	2.825	2.074	2.335	2.400	5.185
Average	Fe	0.231	2.902	2.164	1.353	2.558	7.028
	p-Fe	0.294	2.864	2.119	1.844	2.479	6.107
Experiment [16]	$\cdots$		3.700	2.510	1.793	2.656	6.000

positrons to the observation level. It was estimated by integrating the differential energy deposit over the cascade curve $N_e(x)$ below the observation level x_{obs}:

$$E_{\text{el.}} = \int_{x_{\text{obs}}}^{\infty} \left(\frac{dE}{dx}\right)_{\text{ion}} \cdot N_e(x)dx$$
$$\simeq 2.2 \times 10^6 \cdot N_e(x_{\text{obs}})$$
$$\times \int_{x_{\text{obs}}}^{\infty} \exp\left(\frac{x_{\text{obs}} - x}{\langle\lambda_N\rangle}\right)dx, \qquad (20)$$

where $\langle\lambda_N\rangle \simeq 240$ g/cm^2. $N_e(x_{\text{obs}})$ is the number of electrons at observational level, which was determined from the relation

$$N_e(x_{\text{obs}}) \simeq \langle N_s(x_{\text{obs}})\rangle - 1.8 \cdot \langle N_\mu(x_{\text{obs}})\rangle, \qquad (21)$$

where $\langle N_s(x_{\text{obs}})\rangle$ and $\langle N_\mu(x_{\text{obs}})\rangle$ are mean values of the total number of responses from all particles and muons with 1 GeV threshold, obtained by integrating of experimentally measured corresponding LDFs [15,16]. The ratio 1.8 accounts the difference between the numbers of muons measured by SSDs and underground detectors with 1 GeV threshold. It was derived from earlier calculations [16] and is roughly agreeable with present simulation.

The energy of muons was measured experimentally:

$$E_\mu = \langle E_{1\mu}\rangle \cdot \langle N_\mu(x_{\text{obs}})\rangle, \qquad (22)$$

where $\langle E_{1\mu}\rangle = 10.6$ GeV, which is the mean energy of a single muon.

From the data given in Table II, averaged over all models, the summary value $E_i + E_{\text{el}} + E_\mu$ amounts to $\simeq 93\%$ from primary energy. The rest of it (ΔE) is not controlled by the

TABLE II.   Energy balance of EAS with $E_0 = 10^{18}$ eV and $\cos\theta = 0.95$ from primary (A) according to CORSIKA [23] simulation and experiment [16].

Model	A	E_γ $(\times 10^{17})$ eV	$E_{\text{ion}}.$ $(\times 10^{17})$ eV	E_{el} $(\times 10^{17})$ eV	E_μ $(\times 10^{17})$ eV	ΔE $(\times 10^{17})$ eV	E_0 $(\times 10^{17})$ eV
QGSJet01d	p	0.806	6.620	1.469	0.517	0.565	9.978
	Fe	0.529	6.660	1.306	0.785	0.798	9.972
QGSJetII-04	p	0.859	6.476	1.474	0.547	0.624	9.980
	Fe	0.582	6.430	1.302	0.844	0.866	9.981
SIBYLL-2.1	p	0.909	6.625	1.523	0.428	0.491	9.976
	Fe	0.528	6.679	1.340	0.702	0.716	9.965
EPOS-LHC	p	0.891	6.412	1.482	0.524	0.657	9.966
	Fe	0.543	6.415	1.305	0.794	0.898	9.955
Average	p	0.866	6.533	1.487	0.504	0.584	9.974
	Fe	0.546	6.531	1.313	0.781	0.820	9.968
	p-Fe	0.706	6.532	1.400	0.643	0.702	9.970
Experiment [16]	$\cdots$		9.287	0.947	0.636	0.860	11.730
New estimation	$\cdots$		7.926	0.947	0.618	0.702	10.190

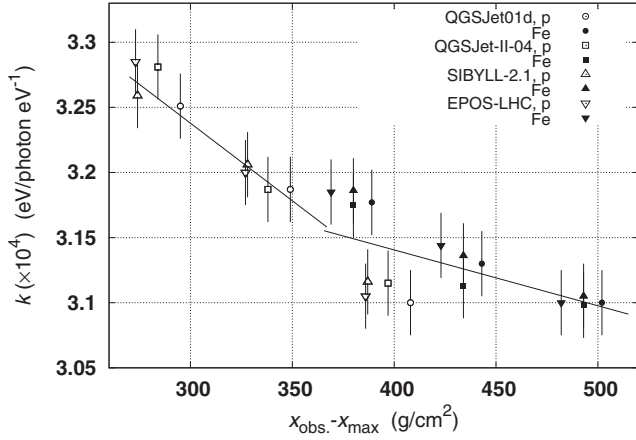FIG. 3. Dependence of the scaling ratio (17) from the path between x_{max} and x_{obs}. for two CR compositions. Lines represent approximations.

array. It includes energy of neutrinos, energy transferred to nuclei in various reactions, and ionization losses of muons and hadrons in the atmosphere. In [15,16], this value was obtained from earlier calculations and is roughly consistent with predictions obtained with CORSIKA.

IV. DISCUSSION

Summary values of all constituents are given in the rightmost column of the Table II. The value $E_0 = 1.173 \times 10^{18}$ eV in the "experiment" column exceeds the mean value $\langle E_0 \rangle = 0.997 \times 10^{18}$ eV obtained in simulation by factor $\simeq 1.177$. This difference is a result of overestimation of the scaling factor k, occurred in [15,16], where it was determined as $k = 3.7 \times 10^4$ eV/photon eV^{-1}, while simulation with CORSIKA gave $\langle k \rangle = 3.157 \times 10^4$ eV/photon eV^{-1}.

The new estimation of primary energy obtained with the use of calorimetric method described above is given in the
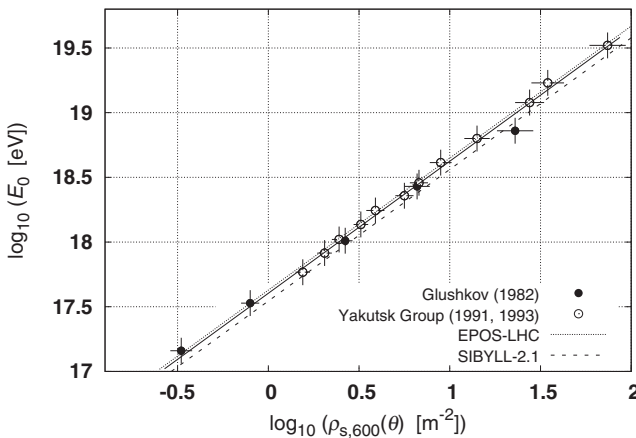

FIG. 4. Energy E_0 reconstructed from the parameter $\rho_{s,600}(\theta)$ in showers with $\langle \cos\theta \rangle = 0.95$. Symbols represent the data given in [16] and [17,18] reprocessed with the new calorimetric estimation. Solid line represents the best fit to all data.
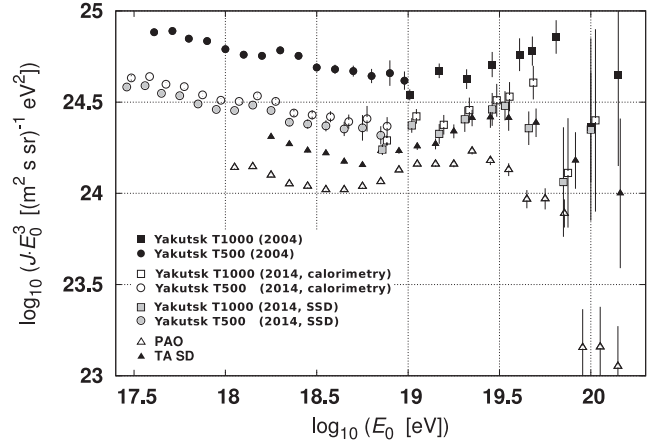

FIG. 5. Differential energy spectrum of CR according to the data from different experiments.

bottom row of the Table II. The value $E_0 = 1.019 \times 10^{18}$ eV was determined with corrected values $E_i = \langle k \rangle \cdot F$, $\langle E_{1\mu} \rangle = 10.3$ GeV, and ΔE. It is shown on Fig. 4 together with other data from [16] with black circles. White circles represent the data from [17,18] reprocessed with the revised values of F and E_{ion}. with the account of the adjusted atmosphere transparency and with introduction of a new scaling factor k (see Fig. 3). A solid line represents the dependency:

$$E_0 = (3.60 \pm 0.3) \times 10^{17} \cdot (\rho_{s,600}(0°))^{1.02\pm0.02}, \quad (23)$$

which describes all of the experimental data when $\rho_{s,600}(18.2°)$ is converted to vertical with the use of (2) with $\lambda_\rho = 415$ g/cm^2. Dotted and dashed lines reflect the relations (11) and (12), which signify limits of the interval containing predictions of all the abovementioned models. The closest to experiment are QGSJet-II-04 and EPOS-LHC, though one cannot exclude the credibility of two others.

In Fig. 5, the CR energy spectra are shown measured by modern giant EAS arrays. Circles and squares (showers selected by master triangles with 500 and 1000 m sides correspondingly) represent the data of the Yakutsk experiment [33]. Energy E_0, estimated with the use of expressions (4) and (5), are shown with black symbols; open symbols represent the same data with energy estimated according to (23), and grey shaded symbols are according to (13). Black triangles represent Telescope Array surface detectors data [34], and white triangles represent PAO [35].

V. CONCLUSION

Application of the CORSIKA code to the Yakutsk EAS array data provided an opportunity to critically examine the experiment's energy calibration which for a long time has been a subject of debates and controversy among our colleagues from other world EAS arrays. This became possible thanks to the availability of modern EAS

development models to a wide range of researchers. With these models we have managed to calculate the responses of scintillation detectors and obtain a set of probable estimations for primary energy (9)–(12). Calculations have revealed that in relations (1) and (4) the energy dissipated in the atmosphere in the form of electromagnetic component was overestimated by 12%–17% depending on the shower maximum $x_{\max}$ (see Fig. 3). This was made worse in (4) due to underestimation of the atmosphere transparency by $\simeq 17\%$. The new calorimetry (23) has led to a lower estimated value of E_0 in comparison with (4) by a factor of $\simeq 1.33$ and in decreased intensity of the CR energy spectrum measured on the Yakutsk EAS array (see Fig. 5).

Independent techniques of E_0 estimation from SSD LDFs (13) and with the use of calorimetric method (23) gave close results, which agree with simulations within 10%–15%. At $E_0 \geq 8 \times 10^{18}$ eV, they do not contradict the TA data [34] and consistently point at the steepening of the primary CR spectrum in the region of extreme energies ($E_0 \geq 3 \times 10^{19}$ eV). This steepening does not contradict to

GZK cutoff but probably has a different astrophysical reason. As for the difference in spectral intensities at $E_0 \leq 8 \times 10^{18}$ eV, it could have other reasons. Probably it is the effect of systematical errors in primary energy reconstruction techniques adopted by different experiments, but one cannot exclude that the said difference is caused by geographical locations of arrays observing different regions of the sky. In [13], such a correlation had been noticed. Our current plan is to continue the elaboration of E_0 estimation at the Yakutsk array with a more detailed analysis of the Cherenkov light data.

ACKNOWLEDGMENTS

[1] K. Greisen, Phys. Rev. Lett. **16**, 748 (1966).

[2] G. T. Zatsepin and V. A. Kuz'min, JETP Lett. **4**, 78 (1966).

[3] R. U. Abbasi, T. Abu-Zayyad, M. Allen, J. F. Amman *et al.* (High Resolution Fly's Eye Collaboration), Phys. Rev. Lett. **100**, 101101 (2008).

[4] J. Abraham, P. Abreu, M. Aglietta, C. Aguirre *et al.* (The Pierre Auger Collaboration), Phys. Rev. Lett. **101**, 061101 (2008).

[5] R. Aloisio, V. Berezinsky, P. Blasi, A. Gazizov, S. Grigorieva, and B. Hnatyk, Astropart. Phys. **27**, 76 (2007).

[6] E. G. Berezhko, S. P. Knurenko, and L. T. Ksenofontov, Astropart. Phys. **36**, 31 (2012).

[7] V. N. Zirakashvili and V. S. Ptuskin, Bull. Russ. Acad. Sci. Phys. **73**, 555 (2009).

[8] D. M. Edge, A. C. Evans, H. J. Garmston, R. J. O. Reid, A. A. Watson, J. G. Wilson, and A. M. Wray, J. Phys. A **6**, 1612 (1973).

[9] A. V. Glushkov, V. M. Grigoriev, M. N. Dyakonov, T. A. Egorov, V. P. Egorova *et al.*, in *Proceedings of 20th ICRC* (Nauka, Moscow, Russia, 1987), Vol. 5, p. 494.

[10] N. Sakaki, M. Chikawa, M. Fukushima, N. Hayashida, K. Honda *et al.*, in *Proceedings of 27th ICRC* (Copernicus, Hamburg, Germany, 2001), Vol. 1, p. 329.

[11] R. U. Abbasi, T. Abu-Zayyad, J. F. Amman, G. C. Archbold, J. A. Bellido *et al.*, Astropart. Phys. **23**, 157 (2005).

[12] J. Abraham, P. Abreu, M. Aglietta, E. J. Ahn, D. Allard *et al.* (Pierre Auger Collaboration), Phys. Lett. B **685**, 239 (2010).

[13] A. V. Glushkov and M. I. Pravdin, JETP Lett. **87**, 345 (2008).

[14] B. R. Dawson, I. C. Maris, M. Roth, F. Salamida *et al.*, EPJ Web Conf. **53**, 01005 (2013).

[15] A. V. Glushkov, V. M. Grigoriev, O. S. Diminshtein, N. N. Efimov, L. I. Kaganov *et al.*, Report of the Institute of Cosmophysical Research and Aeronomy, Yakutsk (1978), A contribution for VI ECRS, Kiel (to be published).

[16] A. V. Glushkov, Ph.D. thesis, SINP MSU (1982) (in Russian).

[17] A. V. Glushkov, M. N. Dyakonov, T. A. Egorov, N. N. Efimov, N. N. Efremov *et al.*, Bull. Acad. Sci. USSR, Phys. Ser. **55**, 713 (1991) (in Russian).

[18] T. A. Egorov (Yakutsk Group), in *Proceedings of the Tokyo Workshop on Techniques for the Study of Extremely High Energy Cosmic Rays* (ICRR, University of Tokyo, 1993) p. 35.

[19] A. V. Glushkov, V. P. Egorova, A. A. Ivanov, S. P. Knurenko, V. A. Kolosov *et al.*, in *Proceedings of the 28th ICRC* (Universal Academy Press, Tokyo, Japan, 2003), Vol. 1, p. 393.

[20] S. I. Nikolsky, in *Proceedings of the 5th International Seminar on Cosmic Rays* (Laboratorio de Física Cósmica de la Universidad Mayor de San Andrés, La Paz, 1962), Vol. 2, p. 48.

[21] N. Budnev, D. Chernov, O. Gress, E. Korosteleva, L. Kuzmichev *et al.*, Astropart. Phys. **50–52**, 18 (2013).

[22] L. G. Dedenko, D. A. Podgrudkov, T. M. Roganova, G. F. Fedorova, E. Y. Fedunin, and G. P. Shozieev, Phys. At. Nucl. **70**, 1759 (2007).

[23] D. Heck, J. Knapp, J. N. Capdevielle, G. Schatz, and T. Thouw, Forschungszentrum Karlsruhe Report No. FZKA 6019, 1998.

[24] A. V. Glushkov, O. S. Diminshtein, T. A. Egorov, N. N. Efimov, L. I. Kaganov *et al.*, in *Collection of Theses* (Yakutia branch of the Acad. Sci. USSR, Yakutsk, 1974), p. 43 (in Russian).

[25] N. N. Kalmykov, S. S. Ostapchenko, and A. I. Pavlov, Nucl. Phys. B, Proc. Suppl. **52**, 17 (1997).

[26] S. Ostapchenko, Phys. Rev. D **83**, 014018 (2011).

[27] E.-J. Ahn, R. Engel, T. K. Gaisser, P. Lipari, and T. Stanev, Phys. Rev. D **80**, 094003 (2009).

[28] T. Pierog, I. Karpenko, J. M. Katzy, E. Yatsenko, and K. Werner, arXiv:1306.0121v2.

[29] G. Battistoni, S. Muraro, P. R. Sala, F. Cerutti, A. Ferrari *et al.*, in *Proceedings of the Hadronic Shower Simulation Workshop 2006*, edited by M. Albrow and R. Raja, Fermilab (AIP Conference Proceeding, New York, 2007), Vol. 896, p. 31.

[30] A. Fassó, A. Ferrari, J. Ranft, and P. R. Sala, Reports No. CERN-2005-10, No. INFN/TC_05/11, and No. SLAC-R-773, 2005.

[31] W. R. Nelson, H. Hirayama, and D. W. O. Rogers, Report No. SLAC 265, Stanford Linear Accelerator Center, 1985.

[32] D. Heck and T. Pierog, *Extensive Air Shower Simulation with CORSIKA: A User's Guide, Version 7.37xx* (Karlsruhe Institut für Technologie, Karlsruhe, 2013).

[33] V. P. Egorova, A. V. Glushkov, A. A. Ivanov, S. P. Knurenko, V. A. Kolosov *et al.*, Nucl. Phys. B, Proc. Suppl. **136**, 3 (2004).

[34] Y. Tsunesada (Telescope Array Collaboration), arXiv: 1111.2507v1.

[35] P. Abreu *et al.* (Pierre Auger Collaboration), arXiv: 1107.4809.